

UC Irvine

UC Irvine Previously Published Works

Title

Identification of biosynthetic precursors for the endocannabinoid anandamide in the rat brain

Permalink

<https://escholarship.org/uc/item/7tp2242x>

Journal

Journal of Lipid Research, 49(1)

ISSN

0022-2275

Authors

Astarita, Giuseppe
Ahmed, Faizy
Piomelli, Daniele

Publication Date

2008

DOI

10.1194/jlr.m700354-jlr200

Supplemental Material

<https://escholarship.org/uc/item/7tp2242x#supplemental>

Copyright Information

This work is made available under the terms of a Creative Commons Attribution License, available at <https://creativecommons.org/licenses/by/4.0/>

Peer reviewed

Identification of biosynthetic precursors for the endocannabinoid anandamide in the rat brain

Giuseppe Astarita,* Faizy Ahmed,[†] and Daniele Piomelli^{1,*§}

Department of Pharmacology and Center for Drug Discovery,* University of California, Irvine, CA 92967; Agilent Technologies,[†] University of California, Irvine/Agilent Analytical Discovery Facility, University of California, Irvine, CA 92967; and Unit of Drug Discovery and Development,[§] Italian Institute of Technology, 16163 Genoa, Italy

Abstract Anandamide is an endogenous signaling lipid that binds to and activates cannabinoid receptors in the brain and peripheral tissues. The endogenous precursors of anandamide, *N*-arachidonoyl phosphatidylethanolamines (NArPEs), are a family of complex glycerophospholipids that derive from the exchange reaction of an arachidonoyl group between the *sn*-1 position of phosphatidylcholine and the primary amine of phosphatidylethanolamine catalyzed by *N*-acyl transferase activity. A precise characterization of the molecular composition of NArPE species generating anandamide has not yet been reported. In the present study, using liquid chromatography coupled to electrospray ionization ion-trap mass spectrometry, we identified the major endogenous NArPE species, which mainly contained *sn*-1 alkenyl groups (C16:0, C18:0, C18:1) and monounsaturated (C18:1) or polyunsaturated (C20:4, C22:4, C22:6) acyl groups at the *sn*-2 position of the glycerol backbone. Using rat brain particulate fractions, we observed a calcium-dependent increase in both NArPEs and anandamide formation after incubation at 37°C for 30 min. Furthermore, a targeted lipidomic analysis showed that Ca²⁺ specifically stimulated the formation of PUFA-containing NArPE species. These results reveal a previously unrecognized preference of brain *N*-acyl transferase activity for polyunsaturated NArPE and provide new insights on the physiological regulation of anandamide biosynthesis.—Astarita, G., F. Ahmed, and D. Piomelli. Identification of biosynthetic precursors for the endocannabinoid anandamide in the rat brain. *J. Lipid Res.* 2008. 49: 48–57.

Supplementary key words fatty acid ethanolamine • arachidonoyl-ethanolamide • *N*-arachidonoyl phosphatidylethanolamines • phosphatidylethanolamine • *N*-acyl phosphatidylethanolamines • *N*-acyl transferase • polyunsaturated fatty acids • phospholipids • lipidomic • nervous system

N-Acyl-substituted derivatives of phosphatidylethanolamines (NAPEs) constitute a family of unusual glycerophospholipids that occur in a wide range of vertebrate animals, including fish (1), reptiles (2), and mammals (3). They are thought to serve as biological precursors for

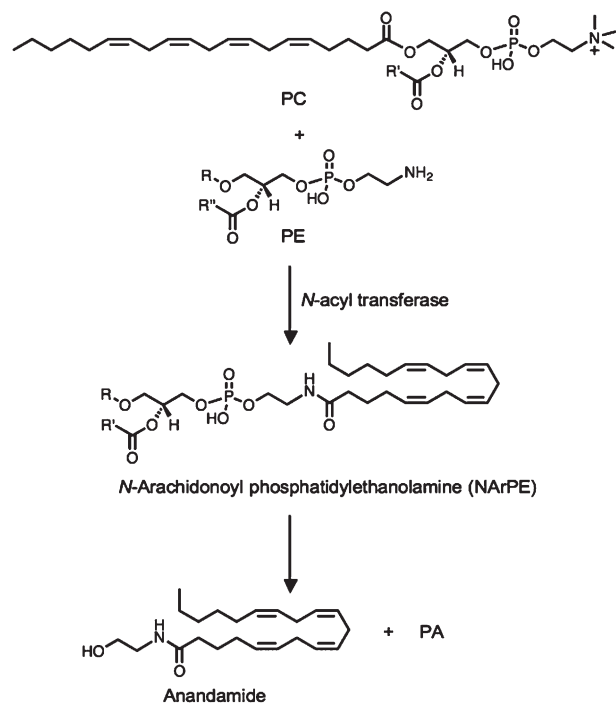
fatty acid ethanolamides (4), a class of signaling lipids involved in critical physiological processes such as pain, feeding, and inflammation (5–7). One of the best-studied fatty acid ethanolamides, arachidonylethanolamide (anandamide), was the first endogenous cannabinoid substance to be identified in the mammalian brain (8). The binding of anandamide to G-protein-coupled cannabinoid receptors exerts a wide range of pharmacological effects that mimic those produced by the active ingredient of *Cannabis*, Δ^9 -tetrahydrocannabinol (9–13). Anandamide is rapidly hydrolyzed to arachidonic acid and ethanolamine by fatty acid amide hydrolases (14), and selective fatty acid amide hydrolase inhibitors have been shown to alleviate pain, anxiety, and depression in rodent models (15–18). However, although much attention has focused on the pharmacological properties and physiological roles of anandamide, much less is known about the biochemical mechanisms responsible for the formation of this endogenous cannabinoid substance.

An important step in understanding the regulation of anandamide biosynthesis in the central nervous system is the complete characterization of its precursors. The proposed mechanism for anandamide biosynthesis in neural cells involves two enzymatic steps (**Scheme 1**): 1) a calcium-dependent *N*-acyl transferase activity, which remains to be molecularly cloned, catalyzes the exchange of an arachidonoyl group between the *sn*-1 position of phosphatidylcholine and the primary amine of phosphatidylethanolamine (PE), leading to the formation of *N*-arachidonoyl phosphatidylethanolamine (NArPE) (3, 19, 20); and 2) a NAPE-specific phospholipase D hydrolyzes the distal phosphodiester bond of NArPE, releasing anandamide (21–24). In addition, NArPEs can generate anandamide through indirect routes, which may involve at least two other NArPE metabolites: *a*) phospho-anandamide generated by the action of a NArPE-specific phospholipase C (25, 26); and *b*) a lyso-NArPE derived from the hydrolysis of NArPE-specific phospholipase A (27–29). However,

Manuscript received 7 August 2007 and in revised form 28 September 2007.

Published, JLR Papers in Press, October 23, 2007
DOI 10.1194/jlr.M700354-JLR200

¹To whom correspondence should be addressed,
e-mail: piomelli@uci.edu



SCHEME 1. Proposed route of anandamide formation in mammalian brain tissue. PA, phosphatidic acid; PC, phosphatidylcholine; PE, phosphatidylethanolamine.

although NArPE is a central component of the biosynthetic pathway leading to anandamide formation, a precise characterization of the molecular composition of this phospholipid in the brain has not yet been reported.

Progress in this area has been hindered by the low brain concentration of NArPE, which represents only a few percentage points of the total phospholipid content (21, 23, 24, 30), as well as by their chemical heterogeneity. Indeed, NArPEs differ not only in the acyl substituents at the *sn*-1, *sn*-2, and *N* positions of PE but also in the nature of the *sn*-1 bond of PE (acyl, alkyl, alkenyl). In the past, resolving these mixtures required multiple analytical steps involving an initial separation of the phospholipid classes by chromatography, followed by serial enzymatic hydrolyses with selective lipases and chromatographic analyses of released products (24, 28, 31–33). Because lipases do not hydrolyze alkenyl- and alkyl-NArPE, chemical methods were used to hydrolyze different *sn*-1 bonds (34, 35). In the present study, we used liquid chromatography (LC) coupled to ion-trap mass spectrometry (MSⁿ), which offers an accurate and sensitive alternative for the analyses of these complex lipids. The aim of the present study was to define the molecular species composition of the endogenous NArPE precursors of anandamide in rat brain and to determine whether calcium stimulation triggers specific changes in their molecular profiles.

MATERIALS AND METHODS

Animals

Adult male Wistar rats (250–300 g) were housed in standard Plexiglas cages at room temperature. A 12 h light/dark cycle was

set with the lights on at 4:45 AM. Water and standard chow pellets (Prolab RMH 2500) were available ad libitum. Rats were anesthetized with halothane and euthanized by decapitation, and the brains were rapidly collected and snap-frozen in liquid N₂. All procedures met National Institutes of Health guidelines for the care and use of laboratory animals and were approved by the Institutional Animal Care and Use Committee of the University of California, Irvine.

Chemicals

We purchased fatty acid chlorides from Nu-Chek Prep (Elysian, MN); 1,2-dipalmitoyl-*sn*-glycero-3-phosphoethanolamine and 1-*O*-hexadecyl-2-palmitoyl-*sn*-glycero-3-phosphoethanolamine-*N*-palmitoyl from Alexis (Lausen, Switzerland); 1-oleoyl-2-palmitoyl-*sn*-glycero-3-phosphoethanolamine-*N*-arachidonoyl, 1-stearoyl-2-arachidonoyl-*sn*-glycero-3-phosphoethanolamine, 1-oleoyl-2-hydroxy-*sn*-glycero-3-phosphoethanolamine, 1-*O*-1'-(*Z*)-octadecenyl-2-oleoyl-*sn*-glycero-3-phosphoethanolamine, and PEs (extracted from porcine brain) from Avanti Polar Lipids (Alabaster, AL); 1-palmitoyl-2-linoleoyl-*sn*-glycero-3-phosphoethanolamine from Sigma-Aldrich (St. Louis, MO); and TLC plates (20 × 20 cm, silica gel 60, 500 mm thick) from Whatman (Clifton, NJ). URB597, synthesized as described (36), was a kind gift from Dr. A. Duranti (University of Urbino, Italy).

Chemical synthesis

We prepared anandamide by the reaction of arachidonoyl chloride with a 10-fold molar excess of ethanolamine (Sigma-Aldrich) or [²H₄]ethanolamine (Cambridge Isotope Laboratories, Andover, MA). Reactions were conducted in dichloromethane at 0–4°C for 15 min with stirring. The products were washed with water, dehydrated over sodium sulfate, filtered, and dried under N₂. They were characterized by LC-MS and ¹H nuclear magnetic resonance spectroscopy. Purity was >98% by LC-MS. NArPEs were prepared by the reaction of fatty acid chlorides with a 2-fold molar excess of PE. Reactions were conducted in dichloromethane at 25°C for 2 h using triethylamine (Sigma-Aldrich) as a catalyst. The products were washed with water, fractionated by silica gel thin-layer chromatography (chloroform-methanol-ammonia, 80:20:2, v/v/v), and characterized by LC-MSⁿ. Purity was >95%.

Lipid extractions

Frozen brains were weighed and homogenized in methanol (1 ml/100 mg tissue) containing [²H₄]anandamide and 1,2-dipalmitoyl-*sn*-glycero-3-phosphoethanolamine-*N*-heptadecanoyl as internal standards. Lipids were extracted with chloroform (2 volumes) and washed with water (1 volume). Organic phases were collected and dried under N₂ and reconstituted in

TABLE 1. Fragmentation patterns of synthetic NAPE species analyzed by direct infusion in ESI-MSⁿ

<i>sn</i> -1, <i>sn</i> -2-NAPE	MS	MS ²	MS ³
		<i>m/z</i>	
16:0–18:2- <i>N</i> 20:4	1,000.8	738.8, 279.3	482, 255
16:0–18:2- <i>N</i> 22:6	1,024.8	762.8, 279.3	506, 255
16:0–18:2- <i>N</i> 18:1	978.8	716.8, 279.3	460, 255
16:0–18:2- <i>N</i> 18:0	980.8	718.8, 279.3	462, 255
18:0–20:4- <i>N</i> 20:4	1,052.8	766.8, 303.3	482, 283
18:0–20:4- <i>N</i> 22:6	1,076.8	790.8, 303.3	506, 283
18:0–20:4- <i>N</i> 18:1	1,030.8	744.8, 303.3	460, 283
18:0–20:4- <i>N</i> 18:0	1,032.8	746.8, 303.3	462, 283
18:1-lyso- <i>N</i> 20:4	—	764.8	482, 281
Plasmenyl 18:0–18:1- <i>N</i> 20:4	1,014.8	750.8, 281.3	403, 482, 267
Alkyl 16:0–16:0- <i>N</i> 16:0	914.8	676.8, 255.3	377, 395

NAPE, *N*-acyl-substituted derivatives of phosphatidylethanolamine.

0.1 ml of chloroform-methanol (1:4, v/v) for LC-MS and LC-MSⁿ analyses.

LC-MS analyses

We quantified anandamide by LC-MS using an 1100-LC system coupled to a 1946D-MS detector (Agilent Technologies, Inc., Palo Alto, CA) equipped with an ESI interface. Anandamide was separated using a XDB Eclipse C18 column (50 × 4.6 mm inner diameter, 1.8 μm; Zorbax) and eluted with a gradient of methanol in water (from 85% to 90% methanol in 2.5 min) at a flow rate of 1.5 ml/min. Column temperature was kept at 40°C. MS detection was in the positive ionization mode, capillary voltage was set at 3 kV, and fragmenter voltage was varied from 120 to 140 V. N₂ was used as drying gas at a flow rate of 13 l/min and a temperature of 350°C. Nebulizer pressure was set at 60 p.s.i. Quantifications were conducted using an isotope dilution method, monitoring the sodium adduct of the molecular ion of anandamide. The limit of quantification was 0.15 pmol.

LC-MSⁿ analyses

We identified and quantified NAPEs by LC-MSⁿ using an 1100-LC system (Agilent Technologies) equipped with an Ion Trap XCT

(Agilent Technologies). NAPEs were separated using a Poroshell 300 SB C18 column (2.1 × 75 mm inner diameter, 5 μm; Agilent Technologies, Wilmington, DE) maintained at 50°C. A linear gradient of methanol in water containing 5 mM ammonium acetate and 0.25% acetic acid (from 85% to 100% of methanol in 4 min) was applied at a flow rate of 1 ml/min. Detection was set in the negative mode, capillary voltage was 4.5 kV, with skim1 at -40 V and capillary exit at -151 V. N₂ was used as drying gas at a flow rate of 12 l/min, with temperature of 350°C and nebulizer pressure of 80 p.s.i. Helium was used as the collision gas. Tissue-derived NAPEs were identified by comparison of their LC retention times and MSⁿ fragmentation patterns with those of authentic standards, prepared as described above. We acquired full-scan MSⁿ spectra of selected NAPE precursor ions by multiple reaction monitoring, with isolation width of 1 and fragmentation voltage of 1.2 V. Ion charge control was on, smart target was set at 50,000 and maximum accumulation time at 50 ms, scan range was 200–1,100 amu, with 26,000 *m/z* per second. Extracted ion chromatograms were used to quantify each NAPE precursor ion by monitoring the characteristic lyso-NAPE product ions in MS² using 1,2-dipalmitoyl-*sn*-glycero-3-phosphoethanolamine-*N*-heptadecanoyl (*m/z* 942.8 > 704.8) as an internal standard. The limit of quantification was 1 pmol [1-*O*-

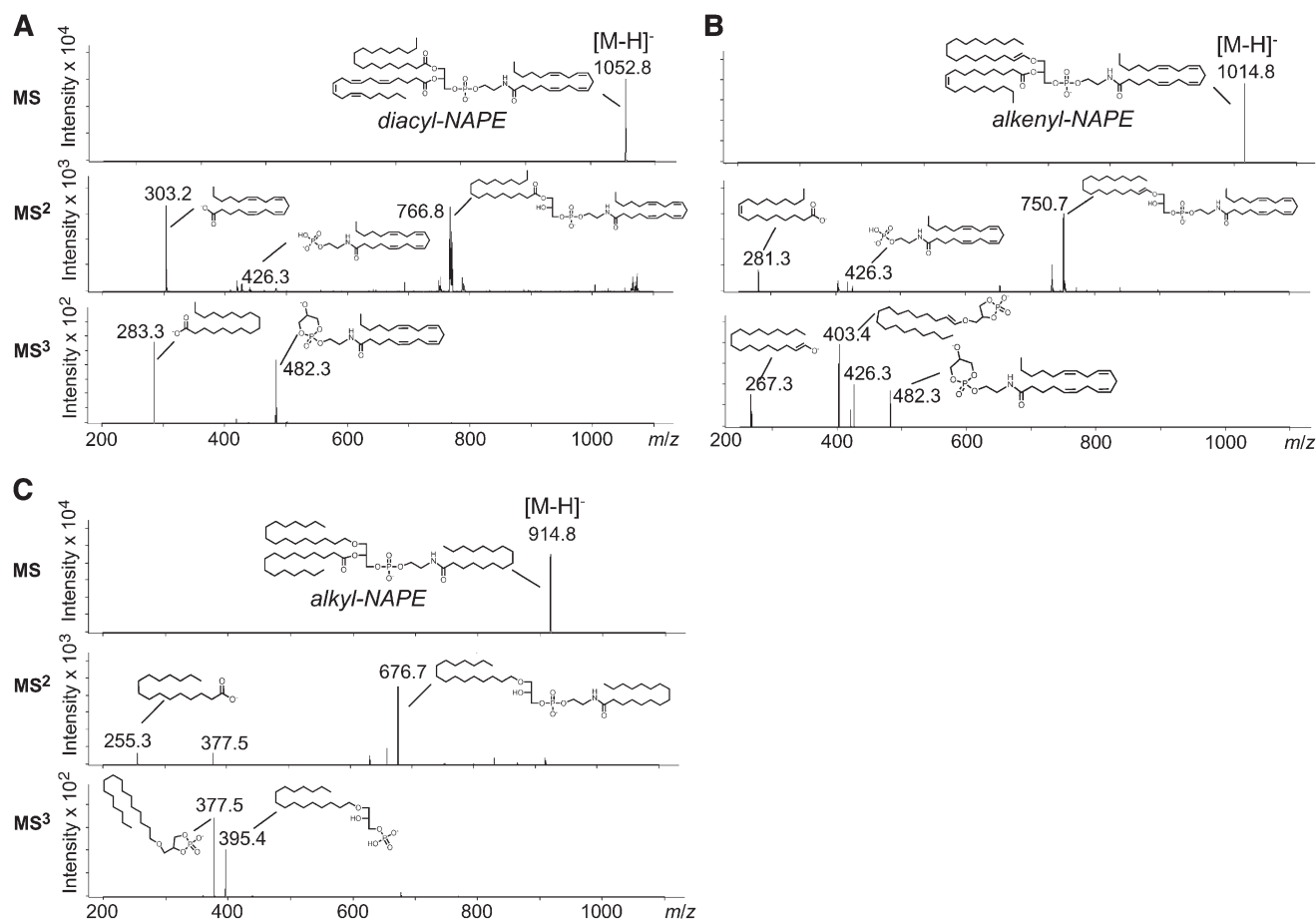


Fig. 1. Fragmentation patterns of various NAPE subclasses by LC-MSⁿ. A, top: Negative-ion electrospray mass spectrum of the representative 1,2-diacyl-NAPE precursor ion (*m/z* 1,052.8) corresponding to the deprotonated 1-stearoyl, 2-arachidonoyl-*sn*-glycero-3-phosphatidylethanolamine-*N*-arachidonoyl. A, center: Collision-induced dissociation (CID) formation of *m/z* 1,052.8. A, bottom: Product ions for CID of the fragment with *m/z* 766.8. B, top: Negative-ion electrospray mass spectra of representative *sn*-1 alkenyl-NAPE (*m/z* 1,014.8) corresponding to the deprotonated 1-*O*-1-(*Z*)-octadecenyl, 2-oleoyl-*sn*-glycero-3-phosphatidylethanolamine-*N*-arachidonoyl. B, center: CID fragments of *m/z* 1,014.8. B, bottom: Productions for CID of the fragment with *m/z* 750.8. C, top: Negative ion electrospray mass spectra of representative *sn*-1 alkyl-NAPE (*m/z* 914.8) corresponding to the deprotonated 1-*O*-hexadecyl-2-palmitoyl-*sn*-glycero-3-phosphoethanolamine-*N*-palmitoyl. C, center: Product ion scan for CID of *m/z* 914.8. C, bottom: Product ions for CID of the fragment with *m/z* 676.8.

1'-(*Z*)-octadecenyl-2-oleoyl-*sn*-glycero-3-phosphoethanolamine-*N*-arachidonoyl, m/z 1,014.8 > 750.8). Lower limits of detection were as follows: 0.04 pmol (alkenyl-NAPE, 1-*O*-1'-(*Z*)-octadecenyl-2-oleoyl-*sn*-glycero-3-phosphoethanolamine-*N*-arachidonoyl), 0.02 pmol (diacyl-NAPE, 1-oleoyl-2-palmitoyl-*sn*-glycero-3-phosphoethanolamine-*N*-arachidonoyl), and 0.05 pmol (alkyl-NAPE, 1-*O*-hexadecyl-2-palmitoyl-*sn*-glycero-3-phosphoethanolamine-*N*-palmitoyl). Detection and analysis were controlled by Agilent/Bruker Daltonics software version 5.2. Processing of MS spectra and bidimensional maps were generated using the MS Processor from Advanced Chemistry Development, Inc. (Toronto, Canada).

In vitro NArPE and anandamide biosynthesis

Fresh brains were collected in ice-cold phosphate-buffered saline (50 mM, pH 7.4), homogenized, and centrifuged at 800 *g* for 15 min and then at 27,000 *g* for 30 min. The 27,000 *g* pellet was suspended in HEPES buffer (50 mM, pH 8.0) and used for the assay. Brain particulate fractions (0.2 mg of protein) were incubated at 37°C for 45 min in HEPES buffer (50 mM, pH 8.0) containing 0.1% Triton X-100 and, when appropriate, 3 mM CaCl₂ or 10 mM EGTA. Incubation was stopped and lipids were extracted by adding chloroform-methanol (2:1, v/v) containing [²H₄]anandamide and 1,2-dipalmitoyl-*sn*-glycero-3-phosphoethanolamine-*N*-heptadecanoyl as internal standards. Lipid extracts were dried under N₂ and reconstituted in chloroform-methanol (1:4, v/v; 0.1 ml) for further analyses.

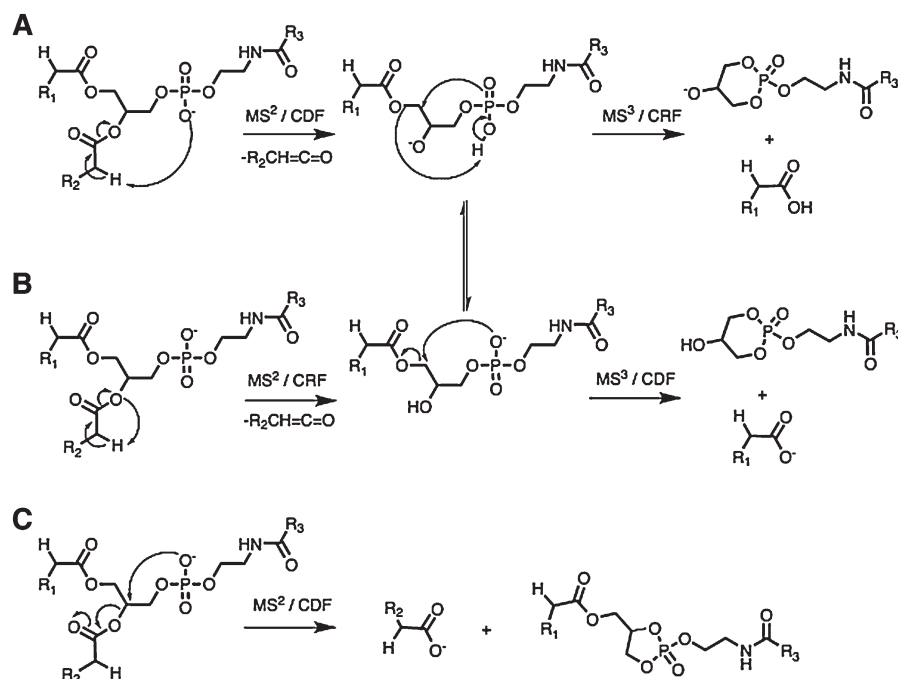
RESULTS

NAPE fragmentation patterns

We analyzed the fragmentation patterns of different molecular species of NAPEs by infusing synthetic standards into the MS ion-trap detector using either negative

or positive ion detection mode (Table 1). When ESI was set in the negative mode, all NAPEs yielded [M-H]⁻ as the predominant pseudomolecular ions, which corresponded to the deprotonation of the phosphate group. All three classes of NAPEs (1-acyl, 1-alkenyl, and 1-alkyl) showed similar ionization efficiencies, as determined by measuring the signal intensities of synthetic standards of known concentration. Collision-induced decomposition (CID) of [M-H]⁻ yielded an abundant product ion identified as *sn*-2 lysophospholipid (Fig. 1), which could derive from a charge-driven (Scheme 2A) or a charge-remote (Scheme 2B) mechanism of fragmentation. Another major MS² fragment was represented by the carboxylate anion derived from position *sn*-2, which could be formed by a charge-driven mechanism involving a nucleophilic attack of the phosphate oxygen on the *sn*-2 glycerol backbone with neutral loss of lyso-NAPEs (Fig. 9C). A minor MS² fragment was identified as *N*-acyl ethanolamide phosphate (Fig. 1A, B).

To identify the fatty acid moiety at position *sn*-1, we further isolated and fragmented (MS³) the *sn*-2 lysophospholipid derived from the CID-MS². Both diacyl-NAPEs (Fig. 1A) and alkenyl-NAPEs (Fig. 1B) yielded primarily two fragments: one distinctive of the *sn*-1 group and the other of the *N*-acyl moiety (Fig. 1A, B). No such fragments were observed for alkyl-NAPEs, suggesting that fragment formation is facilitated by the presence of a carboxyl group or double bond vicinal to the oxygen at the *sn*-1 position. However, both alkyl-NAPEs and alkenyl-NAPEs produced as major product ions in MS³ the lysophosphatidic acid derivatives, which have cyclic phosphate at the *sn*-2 and *sn*-3 positions of the glycerol backbone (Fig. 1B, C) and represent a derivative of cyclic phosphatidic acid (37).



SCHEME 2. Hypothetical fragmentation mechanisms for CID of 1,2-diacyl-*sn*-glycero-3-phosphoethanolamine-*N*-acyl using the ion-trap instrument. In negative ESI, CID-MS² gave both lyso-NAPE (for *N*-acyl-substituted derivatives of phosphatidylethanolamine) (A) and carboxylate anions corresponding to the *sn*-2 fatty acyl group (C); CID-MS³ generated both *N*-acyl cyclic phosphate anions (A) and anions containing the *sn*-1 fatty moiety (B). CDF, collision-driven fragmentation; CRF, collision-remote fragmentation.

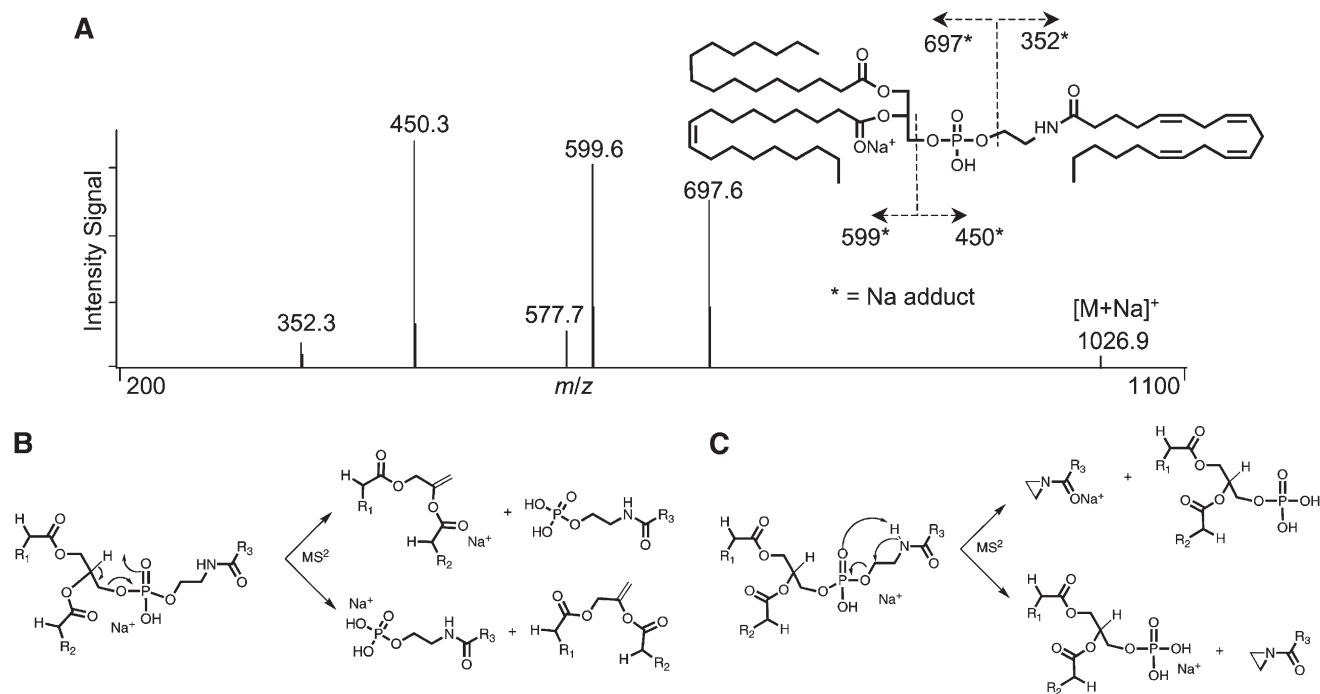


Fig. 2. A: Product ion scan (MS^2) of a representative synthetic diacyl-NAPE sodium adduct ion (1-palmitoyl, 2-oleoyl-*sn*-glycerophosphoethanolamine-*N*-arachidonoyl, $[M+Na]^+$, m/z 1,026.6) in positive detection mode. B, C: Proposed fragmentation mechanisms for CID of the sodium adduct of NAPE using an ion-trap instrument.

When ESI was set in the positive mode, CID of the sodium adduct $[M+Na]^+$ (**Fig. 2A-C**) yielded several fragments, which could derive either from the loss of the *N*-acyl ethanolamide phosphate moiety (**Fig. 2B**) or from the loss of *N*-acyl aziridine (**Fig. 2C**) (38). Although this set of ions provides useful information to define the NAPE species as carrying the *N*-arachidonoyl moiety, it does not allow for precise determination of the fatty acyl groups present on the glycerol backbone. Therefore, we next used the negative ESI mode to determine the exact fatty acid composition of brain NAPE species.

LC separation of NAPEs

A method to characterize synthetic NAPE molecular species by direct infusion into the mass detector was reported previously (39). However, although this analytical approach may help to study the ionization processes and fragmentation patterns of synthetic NAPEs, it is not suitable for the analyses of NAPEs in a complex biological matrix such as brain tissue. Endogenous NAPE species are not easily identifiable by direct infusion into a mass detector for two main reasons: 1) several NAPE species have identical molecular weights; and 2) NAPE represent only

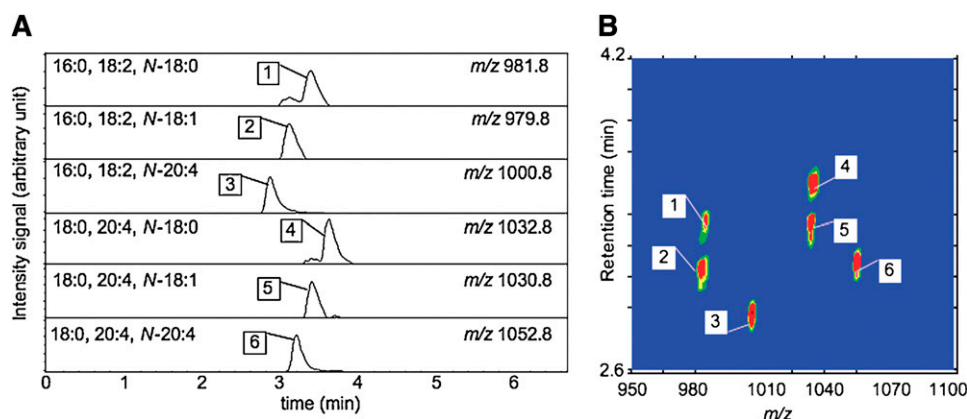


Fig. 3. LC-MS separation of standard NAPE species. A: Representative monodimensional LC-MS extracted ion chromatograms of various NAPE species. Chromatographic conditions are described in Materials and Methods. B: Representative bidimensional LC-MS contour map representation of synthetic NAPE species. The first dimension is elution time, and the second dimension is m/z . The pseudocolor density distribution represents the relative intensity of the signal. Each number denotes an individual pseudomolecular ion $[M-H]^-$ presented in A.

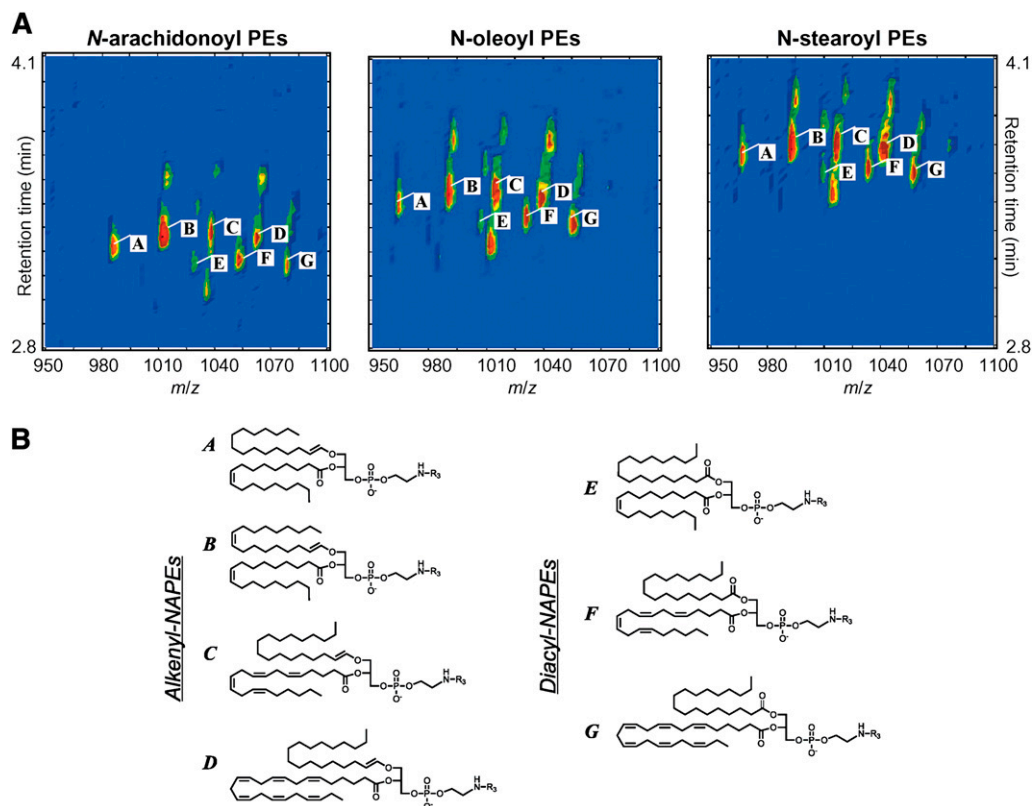


Fig. 4. A: Molecular composition of semisynthetic *N*-arachidonoyl phosphatidylethanolamine (NArPE; left), *N*-oleoyl PE (center), and *N*-stearoyl PE (right) species derived from the reaction of porcine brain PEs with fatty acid chlorides. B: Uppercase letters (A-G) denote individual pseudomolecular ions $[M-H]^-$ for the major glycerol backbone structures of NArPEs.

minor components of the total brain lipid content. Both problems lead to a decrease in sensitivity and to ion suppression effects. Therefore, to simplify the identification process, we separated NAPEs chromatographically, using a combination of high flow velocity (1 ml/min), high temperature (50°C), and a reverse-phase column composed of a thin layer of porous silica (0.25 mm) on a solid core of silica (Poroshell 300 SBC-18) (40–42). These chromatographic conditions minimized the diffusion distances for eluting NAPEs, resulting in sharp peaks and short elution times (<5 min). NAPE species were separated both by chain length and by degree of unsaturation of their fatty acid chains (Fig. 3A). NAPE species containing shorter or more unsaturated acyl chains eluted earlier than those with longer and more saturated chains. Although we were able to separate NAPEs different by a single acyl chain (Fig. 3A), the combinatorial nature of this lipid class made possible only a partial separation of the isomeric species. To obtain a more complete resolution, we coupled LC separation with MS data, representing LC-MS chromatograms as bidimensional maps of NAPE species (LC elution time vs. m/z) (Fig. 3B).

Semisynthetic NAPEs

To generate a library of LC-MSⁿ data on NAPEs, we prepared sets of NAPEs by separately reacting commer-

cially available PE extracted from porcine brain with different acyl chlorides (18:0, 18:1 Δ^9 , 20:4 $\Delta^{5,8,11,14}$). Each NAPE was identified by MSⁿ, acquiring full-scan LC-MS² and MS³ spectra of selected precursor ions. LC-MS data

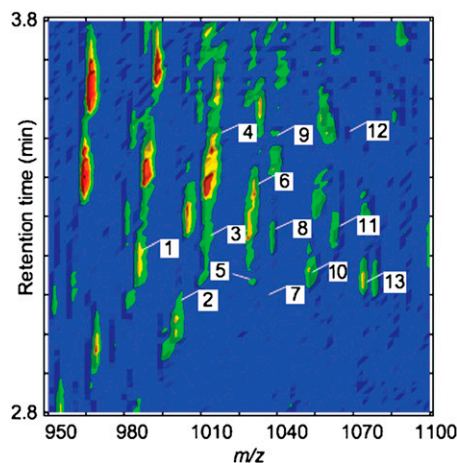


Fig. 5. Bidimensional LC-MS contour map of endogenous NArPE species in rat brain. The first dimension is elution time, and the second dimension is m/z . The colored density distribution represents the relative intensity of the signal. Numbers (1–13) denote individual pseudomolecular ions $[M-H]^-$ for anandamide-generating NArPEs as identified in Table 2.

TABLE 2. Fatty acid composition, ESI-MSⁿ identification, brain levels, and relative amounts of the major anandamide-generating NArPE species detected in rat brain

NArPE Identifier	NArPE <i>sn-1,sn-2</i>	MS	MS ²	MS ³	NArPE	NArPE
			<i>m/z</i>		<i>pmol/g wet tissue</i>	%
1	p16:0, 18:1	986.8	722.8, 281.3	239, 375, 482.6	66 ± 10	8.1
2	16:0, 18:1	1,002.8	738.8, 281.3	255, 482.6	57 ± 11	7.0
3	p18:1, 18:1	1,012.8	748.8, 281.3	265, 401, 482.6	130 ± 18	16.0
4	p18:0, 18:1	1,014.8	750.8, 281.3	267, 403, 482.6	86 ± 11	10.6
5	18:1, 18:1	1,028.8	764.8, 281.3	281, 482.6	27 ± 15	3.3
6	18:0, 18:1	1,030.8	766.8, 281.3	283, 482.6	82 ± 10	10.1
7	p18:1, 20:4	1,034.8	748.8, 303.3	265, 401, 482.6	62 ± 9	7.6
8a	p18:0, 20:4	1,036.8	750.8, 303.3	267, 403, 482.6	22 ± 7	2.7
8b	p16:0, 22:4	1,036.8	722.8, 331.3	239, 375, 482.6	60 ± 9	7.3
9	p18:1, 20:1	1,040.8	748.8, 309.3	265, 401	8 ± 2	1.0
10	18:0, 20:4	1,052.8	766.8, 303.3	283, 482.6	66 ± 8	8.1
11	p18:0, 22:6	1,060.8	750.8, 327.3	267, 403, 482.6	26 ± 6	3.2
—	p18:1, 22:4	1,062.8	748.8, 331.3	265, 482.6	7 ± 2	0.8
12	p18:0, 22:4	1,064.8	750.8, 331.3	267, 482.6	59 ± 12	7.2
—	p18:1, 22:1	1,068.8	748.8, 337.3	265.3, 482.6	6 ± 2	0.7
13	18:0, 22:6	1,076.8	766.8, 327.3	283, 482.6	51 ± 11	6.3
—	18:0, 22:5	1,078.8	766.8, 329.3	283, 482.6	traces	—
—	18:0, 22:4	1,080.8	766.8, 331.3	283.3, 482.6	traces	—

NArPE, N-arachidonoyl phosphatidylethanolamine. NArPE results are expressed as means ± SEM of three different brains.

obtained with these semisynthetic NArPEs were represented as bidimensional maps (Fig. 4A), which allowed us to attribute unambiguous coordinates to each molecular species. In such maps, we could intuitively distinguish repetitive patterns of fatty acyl glycerol backbones (Fig. 4A), which predictably shifted along the retention time and *m/z* axes according to their chemical structures (Fig. 4B).

Identification of NArPEs in rat brain

NArPEs extracted from rat brain eluted from the column in a narrow time window (2.8–3.8 min) as a complex mixture of isobaric and isomeric molecular species. As shown in Fig. 5, however, a bidimensional representation offered a clear snapshot of the NArPE profile. It was possible to recognize longitudinal clusters of spots for alkenyl-NArPEs separated by a difference of 28 mass units (one ethylene group). In each longitudinal cluster, mass peaks with 2 mass unit differences were attributable to the presence of unsaturation. We were also able to identify the intervening lower cluster of peaks, which have mass differences of 16 from the corresponding alkenyl-NArPE species, as diacyl-NArPE species. In total, we found that

alkenyl-NArPEs constitute ~65% of the NArPE in the rat brain (Table 2). Diacyl-NArPEs constitute the remaining 35%, with only trace amounts of alkyl-NArPEs being detected. In particular, we identified 13 major endogenous NArPEs, which mainly contained *sn-1* alkenyl groups (C16:0, C18:0, C18:1) and monounsaturated (C18:1) or polyunsaturated (C20:4, C22:4, C22:6) *sn-2* acyl groups (Table 2). Notably, the *sn-1* C18:1 moiety was predominant in alkenyl-NArPE species containing more saturated fatty acids at the *sn-2* position (Table 2).

In vitro NArPE and anandamide biosynthesis

Increases in intracellular Ca²⁺ ion concentrations in neurons stimulate NArPE and anandamide biosynthesis (22, 24, 43). To identify the NArPE species produced by Ca²⁺ stimulation, we incubated brain particulate fractions (27,000 g) with either CaCl₂ (3 mM) or EGTA (10 mM) and measured NArPE formation by LC-MS. We observed a marked increase in high molecular weight NArPE species in Ca²⁺-stimulated fractions compared with EGTA-treated fractions (Fig. 6A, B) or with unstimulated rat brain extracts (Fig. 5). A targeted lipidomic analysis showed that

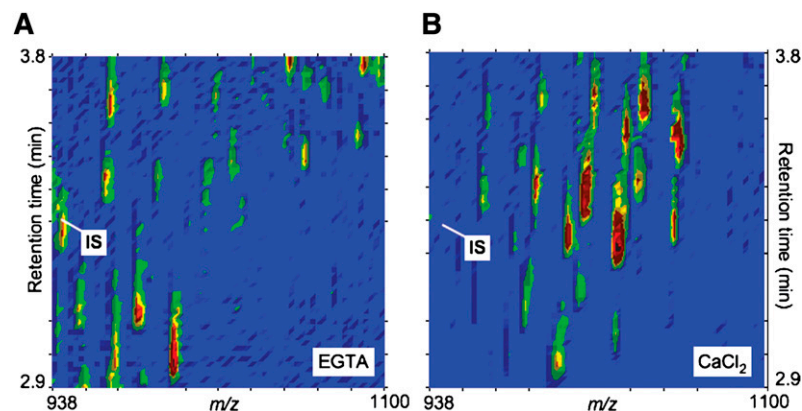


Fig. 6. Bidimensional LC-MS contour maps of endogenous NArPE species derived from incubation of rat brain particulate fractions in the presence of either EGTA (10 mM) (A) or CaCl₂ (3 mM) (B), as reported in Materials and Methods. The first dimension is elution time, and the second dimension is *m/z*. The colored density distribution represents the relative intensity of the signal. Note that NArPE levels may be compared with the signal intensity of the internal standard (IS; *m/z* 942.8).

TABLE 3. Fold increase in NArPE molecular species after incubating brain particulate fractions with CaCl₂ (3 mM) or EGTA (10 mM)

NArPE Identifier	NArPE <i>sn-1,sn-2</i>	NArPE _(Ca²⁺/EGTA)	NArPE Identifier	NArPE <i>sn-1,sn-2</i>	NArPE _(Ca²⁺/EGTA)
			<i>fold increase</i>		<i>fold increase</i>
1	p16:0, 18:1	0.6 ± 0.4	9	p18:1, 20:1	-0.5 ± 0.5
2	16:0, 18:1	0.8 ± 0.5	10	18:0, 20:4	8.9 ± 1.2
3	p18:1, 18:1	1.0 ± 0.6	11	p18:0, 22:6	7.9 ± 0.8
4	p18:0, 18:1	0.5 ± 0.5	—	p18:1, 22:4	14.7 ± 1.4
5	18:1, 18:1	0.2 ± 0.4	12	p18:0, 22:4	6.4 ± 2.0
6	18:0, 18:1	-0.2 ± 0.3	—	p18:1, 22:1	nd
7	p18:1, 20:4	6.7 ± 0.5	13	18:0, 22:6	11.2 ± 0.6
8a	p18:0, 20:4	7.5 ± 0.8	—	18:0, 22:5	nd
8b	p16:0, 22:4	7.4 ± 0.4	—	18:0, 22:4	nd

nd, not detectable. Results are expressed as means ± SEM of three separate experiments (n = 6–9).

Ca²⁺ incubation specifically stimulated the formation of the NArPE species containing polyunsaturated acyl groups at the *sn-2* position of the glycerol backbone. In particular, we identified an 8.84 ± 0.9-fold increase in NArPE species containing PUFAs (C20:4, C22:6, C22:4) compared with a 0.34 ± 0.4-fold increase in NArPE species containing monounsaturated fatty acids (C18:1, C20:1) (Table 3). Furthermore, after Ca²⁺ incubation, we were also able to detect new NArPE species with PUFAs at the *sn-2* position, such as 16:0,20:4 (*m/z* 1,024.8 > 738.8), p16:0, 20:4 (*m/z* 1,008.8 > 722.8), and 16:0,22:4 (*m/z* 1,052.8 > 738.8), which were undetectable otherwise (not listed in Tables 2, 3). Finally, we examined the effect of Ca²⁺ incubation on the levels of one of the main anandamide-generating NArPEs (1-stearoyl, 2-docosahexaenoyl-*sn*-glycero-3-phosphoethanolamine-*N*-arachidonoyl) and anandamide. We found that the levels of both lipids were enhanced by Ca²⁺ (Fig. 7A, B). Furthermore, the Ca²⁺-induced increases in anandamide levels were further amplified when particulate fractions were incubated in the presence of the fatty acid amide hydrolase inhibitor URB597 (Fig. 7B).

DISCUSSION

NArPEs are the biological precursors for anandamide, an endogenous signaling lipid that binds to and activates cannabinoid receptors in the brain and peripheral tissues (8). In the present study, we developed an integrated LC-MS approach that allowed us 1) to characterize the precise molecular composition of NArPE species in the rat brain and 2) to demonstrate that Ca²⁺ potently enhances the formation of a subset of such species, presumably through the stimulation of a selective *N*-acyl transferase activity.

NArPEs offered a clear and reproducible fragmentation pattern in ESI-MSⁿ, which was characterized by the formation of a lyso-NArPE and *sn-2* carboxylate anion in MS² and by *sn-1* fatty acid and *N*-acyl cyclic phosphate derivatives in MS³. These results are in agreement with previous studies showing that CID-MS² of PEs yields *sn-2* lysophospholipids as the most prominent fragments, probably through a charge-remote fragmentation process (44). An alternative mechanism of fragmentation for the formation of the lysophospholipid anions, which involved

charge-driven fragmentation, has been proposed as a minor reaction pathway in CID-MS² of triple quadrupole instruments (45, 46). Therefore, the interpretation of our mass spectra suggests that a combination of the two mechanisms of fragmentation could lead to the generation of the fragment ions observed in MS² and MS³. Notably, this fragmentation pattern allowed us to distinguish the *sn-1* fatty acid moiety (alkyl, alkenyl, or acyl) NArPE species without the need of further purification of the lipids.

Our results on the NArPE composition in rat brain extracts are in agreement with previous studies showing that 1) bovine brain contains a mixture of diacyl- and alkenyl-NArPE species in a ratio of 2:3 (47) and 2) dog brain contains a mixture of diacyl-, alkenyl-, and alkyl-NArPEs of 50, 45, and 5%, respectively (3, 23) (note that in these analyses, gross NAPE levels were measured). Although the significance of these different ratios of alkenyl-NArPE over diacyl-NArPE remains unknown, we recently reported that in intestinal mucosa, diacyl-NArPE species constitute almost the totality of NArPE species, whereas intestinal

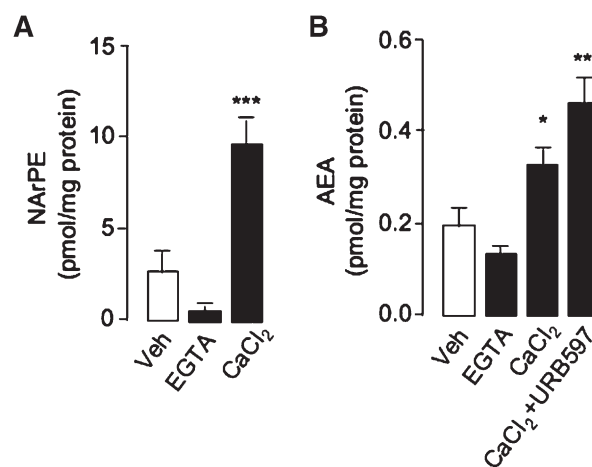



Fig. 7. Effects of various treatments on the levels of NArPE 1-stearoyl, 2-docosahexaenoyl-*sn*-glycero-3-phosphoethanolamine-*N*-arachidonoyl (*m/z* 1,076.8 > 766.8) (A) and anandamide (AEA; *m/z* 370.3) (B) in rat brain particulate fractions incubated at 37°C for 30 min. Veh, vehicle (50 mM HEPES, pH 8.0, 10 mM EGTA, 3 mM CaCl₂, and 100 nM URB 597). Results are expressed as means ± SEM (n = 6–9). **P* < 0.05, ***P* < 0.01, ****P* < 0.001 versus vehicle by Student's *t*-test.

serosa contains comparable amounts of alkenyl-NArPE and diacyl-NArPE (48), suggesting that NArPE composition may be linked to a not yet characterized biological function. For example, it has been reported that plasmalogenes have a larger dipole moment and form hexagonal phases at lower temperatures than the diacyl-PE analogs, indicating that they could be involved in membrane fluidity and facilitate the membrane fusion process (49). Therefore, it can be hypothesized that NArPE composition may affect the physical properties of membrane domains (50, 51) and that the ratio of diacyl-NArPEs over alkenyl-NArPEs may have an influence on the signaling processes in the brain.

Another part of our study offered a more dynamic picture of what may happen to NArPEs in the brain after Ca^{2+} stimulation. In neurons, Ca^{2+} triggers the activation of many enzymes involved in lipid metabolism, such as phospholipases and acyl transferase, with the subsequent generation of novel lipid molecules. In particular, it has been reported that NArPEs accumulate in neuronal tissue in response to the intracellular increase in Ca^{2+} ion concentration (22, 24) under both physiological and pathological conditions, such as in ischemic rat brain (52), glutamate (19, 30), and sodium azide-induced and kainate neurotoxicity (53, 54), and in models of rat brain necrosis (30, 55). Our study shows that the Ca^{2+} -dependent pathway for anandamide biosynthesis specifically involves the formation of NArPE species containing polyunsaturated fatty acid groups (mainly 20:4 and 22:6) at the *sn*-2 position of the glycerol backbone. NArPE species containing more saturated fatty acid species, although present in brain tissue, appear to be less sensitive to Ca^{2+} stimulation. This result reveals a previously unrecognized preference of brain *N*-acyl transferase activity for polyunsaturated NArPE. Such a preference might derive either from a substrate selectivity of the *N*-acyl transferase toward polyunsaturated PE species or from a localization of this enzyme in membrane domains enriched in PUFA-containing PE (51, 56). Finally, irrespective of the biosynthetic pathways involved (3, 19–29), the fact that NArPE and anandamide levels increase in parallel supports a metabolic precursor-product relationship between these lipids. In conclusion, the identification of NArPE species in the rat brain provides useful new insights into the physiological regulation of anandamide biosynthesis. 

The contribution of the Agilent Technologies/University of California, Irvine Analytical Discovery Facility, Center for Drug Discovery is gratefully acknowledged. This work was supported by grants from the Agilent Foundation and the National Institutes of Health (DA-022702 and DA-012413 to D.P.).

REFERENCES

- Chapman, K. D. 2000. Emerging physiological roles for *N*-acylphosphatidylethanolamine metabolism in plants: signal transduction and membrane protection. *Chem. Phys. Lipids*. **108**: 221–229.
- Astarita, G., B. C. Rourke, J. B. Andersen, J. Fu, J. H. Kim, A. F. Bennett, J. W. Hicks, and D. Piomelli. 2006. Postprandial increase of oleylethanolamide mobilization in small intestine of the Burmese python (*Python molurus*). *Am. J. Physiol. Regul. Integr. Comp. Physiol.* **290**: R1407–R1412.
- Schmid, H. H., P. C. Schmid, and V. Natarajan. 1990. *N*-Acylated glycerophospholipids and their derivatives. *Prog. Lipid Res.* **29**: 1–43.
- Schmid, H. H. 2000. Pathways and mechanisms of *N*-acylethanolamine biosynthesis: can anandamide be generated selectively? *Chem. Phys. Lipids*. **108**: 71–87.
- Schmid, H. H., and E. V. Berdyshev. 2002. Cannabinoid receptor-inactive *N*-acylethanolamines and other fatty acid amides: metabolism and function. *Prostaglandins Leukot. Essent. Fatty Acids*. **66**: 363–376.
- Calignano, A., G. La Rana, and D. Piomelli. 2001. Antinociceptive activity of the endogenous fatty acid amide, palmitylethanolamide. *Eur. J. Pharmacol.* **419**: 191–198.
- Rodríguez de Fonseca, F., M. Navarro, R. Gómez, L. Escuredo, F. Nava, J. Fu, E. Murillo-Rodríguez, A. Giuffrida, J. LoVerme, S. Gaetani, et al. 2001. An anorexic lipid mediator regulated by feeding. *Nature*. **414**: 209–212.
- Devane, W. A., L. Hanus, A. Breuer, R. G. Pertwee, L. A. Stevenson, G. Griffin, D. Gibson, A. Mandelbaum, A. Etinger, and R. Mechoulam. 1992. Isolation and structure of a brain constituent that binds to the cannabinoid receptor. *Science*. **258**: 1946–1949.
- Felder, C. C., E. M. Briley, J. Axelrod, J. T. Simpson, K. Mackie, and W. A. Devane. 1993. Anandamide, an endogenous cannabimimetic eicosanoid, binds to the cloned human cannabinoid receptor and stimulates receptor-mediated signal transduction. *Proc. Natl. Acad. Sci. USA*. **90**: 7656–7660.
- Crawley, J. N., R. L. Corwin, J. K. Robinson, C. C. Felder, W. A. Devane, and J. Axelrod. 1993. Anandamide, an endogenous ligand of the cannabinoid receptor, induces hypomotility and hypothermia in vivo in rodents. *Pharmacol. Biochem. Behav.* **46**: 967–972.
- McGregor, I. S., J. C. Arnold, M. F. Weber, A. N. Topple, and G. E. Hunt. 1998. A comparison of Δ^9 -THC and anandamide induced *c-fos* expression in the rat forebrain. *Brain Res.* **802**: 19–26.
- Tsou, K., M. I. Nogueiron, S. Muthian, M. C. Sañudo-Peña, C. J. Hillard, D. G. Deutsch, and J. M. Walker. 1998. Fatty acid amide-hydrolase is located preferentially in large neurons in the rat central nervous system as revealed by immunohistochemistry. *Neurosci. Lett.* **254**: 137–140.
- Thomas, E. A., B. F. Cravatt, P. E. Danielson, N. B. Gilula, and J. G. Sutcliffe. 1997. Fatty acid amide hydrolase, the degradative enzyme for anandamide and oleamide, has selective distribution in neurons within the rat central nervous system. *J. Neurosci. Res.* **50**: 1047–1052.
- Cravatt, B. F., D. K. Giang, S. P. Mayfield, D. L. Boger, R. A. Lerner, and N. B. Gilula. 1996. Molecular characterization of an enzyme that degrades neuromodulatory fatty-acid amides. *Nature*. **384**: 83–87.
- Gaetani, S., V. Cuomo, and D. Piomelli. 2003. Anandamide hydrolysis: a new target for anti-anxiety drugs? *Trends Mol. Med.* **9**: 474–478.
- Kathuria, S., S. Gaetani, D. Fegley, F. Valino, A. Duranti, A. Tontini, M. Mor, G. Tarzia, G. La Rana, A. Calignano, et al. 2003. Modulation of anxiety through blockade of anandamide hydrolysis. *Nat. Med.* **9**: 76–81.
- Connell, K., N. Bolton, D. Olsen, D. Piomelli, and A. G. Hohmann. 2006. Role of the basolateral nucleus of the amygdala in endocannabinoid-mediated stress-induced analgesia. *Neurosci. Lett.* **397**: 180–184.
- Gobbi, G., F. R. Bambico, R. Mangieri, M. Bortolato, P. Campolongo, M. Solinas, T. Cassano, M. G. Morgese, G. Debonnel, A. Duranti, et al. 2005. Antidepressant-like activity and modulation of brain monoaminergic transmission by blockade of anandamide hydrolysis. *Proc. Natl. Acad. Sci. USA*. **102**: 18620–18625.
- Hansen, H. S., L. Lauritzen, B. Moesgaard, A. M. Strand, and H. H. Hansen. 1998. Formation of *N*-acyl-phosphatidylethanolamines and *N*-acylethanolamines: proposed role in neurotoxicity. *Biochem. Pharmacol.* **55**: 719–725.
- Schmid, H. H., P. C. Schmid, and V. Natarajan. 1996. The *N*-acylation-phosphodiesterase pathway and cell signalling. *Chem. Phys. Lipids*. **80**: 133–142.
- Sugiura, T., S. Kondo, A. Sukagawa, T. Tonegawa, S. Nakane, A. Yamashita, Y. Ishima, and K. Waku. 1996. Transacylase-mediated and phosphodiesterase-mediated synthesis of *N*-arachidonylethanolamine, an endogenous cannabinoid-receptor ligand, in rat brain microsomes. Comparison with synthesis from free arachidonic acid and ethanolamine. *Eur. J. Biochem.* **240**: 53–62.

22. Natarajan, V., P. C. Schmid, and H. H. Schmid. 1986. *N*-Acylethanolamine phospholipid metabolism in normal and ischemic rat brain. *Biochim. Biophys. Acta.* **878**: 32–41.
23. Natarajan, V., P. C. Schmid, P. V. Reddy, M. L. Zuzarte-Augustin, and H. H. Schmid. 1983. Biosynthesis of *N*-acylethanolamine phospholipids by dog brain preparations. *J. Neurochem.* **41**: 1303–1312.
24. Cadas, H., E. di Tomaso, and D. Piomelli. 1997. Occurrence and biosynthesis of endogenous cannabinoid precursor, *N*-arachidonoyl phosphatidylethanolamine, in rat brain. *J. Neurosci.* **17**: 1226–1242.
25. Liu, J., L. Wang, J. Harvey-White, D. Osei-Hyiaman, R. Razdan, Q. Gong, A. C. Chan, Z. Zhou, B. X. Huang, H. Y. Kim, et al. 2006. A biosynthetic pathway for anandamide. *Proc. Natl. Acad. Sci. USA.* **103**: 13345–13350.
26. Liu, J., L. Wang, J. Harvey-White, B. X. Huang, H. Y. Kim, S. Luquet, R. D. Palmiter, G. Krystal, R. Rai, A. Mahadevan, et al. 2007. Multiple pathways involved in the biosynthesis of anandamide. *Neuropharmacology*. In press.
27. Sun, Y. X., K. Tsuboi, Y. Okamoto, T. Tonai, M. Murakami, I. Kudo, and N. Ueda. 2004. Biosynthesis of anandamide and *N*-palmitoylethanolamine by sequential actions of phospholipase A2 and lysophospholipase D. *Biochem. J.* **380**: 749–756.
28. Leung, D., A. Saghatelian, G. M. Simon, and B. F. Cravatt. 2006. Inactivation of *N*-acyl phosphatidylethanolamine phospholipase D reveals multiple mechanisms for the biosynthesis of endocannabinoids. *Biochemistry.* **45**: 4720–4726.
29. Simon, G. M., and B. F. Cravatt. 2006. Endocannabinoid biosynthesis proceeding through glycerophospho-*N*-acyl ethanolamine and a role for alpha/beta-hydrolase 4 in this pathway. *J. Biol. Chem.* **281**: 26465–26472.
30. Hansen, H. S., B. Moesgaard, H. H. Hansen, A. Schousboe, and G. Petersen. 1999. Formation of *N*-acyl-phosphatidylethanolamine and *N*-acylethanolamine (including anandamide) during glutamate-induced neurotoxicity. *Lipids.* **34**(Suppl.): 327–330.
31. Hansen, H. S., B. Moesgaard, H. H. Hansen, and G. Petersen. 2001. When and where are *N*-acylethanolamine phospholipids and anandamide formed? *World Rev. Nutr. Diet.* **88**: 223–227.
32. Petersen, G., C. Sorensen, P. C. Schmid, A. Artmann, M. Tang-Christensen, S. H. Hansen, P. J. Larsen, H. H. Schmid, and H. S. Hansen. 2006. Intestinal levels of anandamide and oleoylethanolamide in food-deprived rats are regulated through their precursors. *Biochim. Biophys. Acta.* **1761**: 143–150 (discussion 141–142).
33. Okamoto, Y., J. Morishita, J. Wang, P. C. Schmid, R. J. Krebsbach, H. H. Schmid, and N. Ueda. 2005. Mammalian cells stably overexpressing *N*-acylphosphatidylethanolamine-hydrolysing phospholipase D exhibit significantly decreased levels of *N*-acylphosphatidylethanolamines. *Biochem. J.* **389**: 241–247.
34. Ramanadham, S., F. F. Hsu, A. Bohrer, W. Nowatzke, Z. Ma, and J. Turk. 1998. Electrospray ionization mass spectrometric analyses of phospholipids from rat and human pancreatic islets and subcellular membranes: comparison to other tissues and implications for membrane fusion in insulin exocytosis. *Biochemistry.* **37**: 4553–4567.
35. Kim, H. Y., T. C. Wang, and Y. C. Ma. 1994. Liquid chromatography/mass spectrometry of phospholipids using electrospray ionization. *Anal. Chem.* **66**: 3977–3982.
36. Mor, M., S. Rivara, A. Lodola, P. V. Plazzi, G. Tarzia, A. Duranti, A. Tontini, G. Piersanti, S. Kathuria, and D. Piomelli. 2004. Cyclohexylcarbamic acid 3'- or 4-substituted biphenyl-3-yl esters as fatty acid amide hydrolase inhibitors: synthesis, quantitative structure-activity relationships, and molecular modeling studies. *J. Med. Chem.* **47**: 4998–5008.
37. Murakami-Murofushi, K., A. Uchiyama, Y. Fujiwara, T. Kobayashi, S. Kobayashi, M. Mukai, H. Murofushi, and G. Tigyi. 2002. Biological functions of a novel lipid mediator, cyclic phosphatidic acid. *Biochim. Biophys. Acta.* **1582**: 1–7.
38. Hsu, F. F., and J. Turk. 2000. Characterization of phosphatidylethanolamine as a lithiated adduct by triple quadrupole tandem mass spectrometry with electrospray ionization. *J. Mass Spectrom.* **35**: 595–606.
39. Hansen, H. H., S. H. Hansen, I. Bjornsdottir, and H. S. Hansen. 1999. Electrospray ionization mass spectrometric method for the determination of cannabinoid precursors: *N*-acylethanolamine phospholipids (NAPEs). *J. Mass Spectrom.* **34**: 761–767.
40. Kirkland, J. J., F. A. Truszkowski, C. H. Dilks, Jr., and G. S. Engel. 2000. Superficially porous silica microspheres for fast high-performance liquid chromatography of macromolecules. *J. Chromatogr. A.* **890**: 3–13.
41. Peterson, B. L., and B. S. Cummings. 2006. A review of chromatographic methods for the assessment of phospholipids in biological samples. *Biomed. Chromatogr.* **20**: 227–243.
42. Barroso, B., and R. Bischoff. 2005. LC-MS analysis of phospholipids and lysophospholipids in human bronchoalveolar lavage fluid. *J. Chromatogr. B Analyt. Technol. Biomed. Life Sci.* **814**: 21–28.
43. Cadas, H., S. Gaillet, M. Beltramo, L. Venance, and D. Piomelli. 1996. Biosynthesis of an endogenous cannabinoid precursor in neurons and its control by calcium and cAMP. *J. Neurosci.* **16**: 3934–3942.
44. Larsen, A., S. Uran, P. B. Jacobsen, and T. Skotland. 2001. Collision-induced dissociation of glycerol phospholipids using electrospray-ion-trap mass spectrometry. *Rapid Commun. Mass Spectrom.* **15**: 2393–2398.
45. Hsu, F. F., and J. Turk. 2000. Charge-remote and charge-driven fragmentation processes in diacyl glycerophosphoethanolamine upon low-energy collisional activation: a mechanistic proposal. *J. Am. Soc. Mass Spectrom.* **11**: 892–899.
46. Pulfer, M., and R. C. Murphy. 2003. Electrospray mass spectrometry of phospholipids. *Mass Spectrom. Rev.* **22**: 332–364.
47. Debuch, H., and G. Wendt. 1967. [On a new group of colamine-rich glycerol phosphatides from brain.] *Hoppe Seylers Z. Physiol. Chem.* **348**: 471–474.
48. Fu, J., G. Astarita, S. Gaetani, J. Kim, B. F. Cravatt, K. Mackie, and D. Piomelli. 2007. Food intake regulates oleoylethanolamide formation and degradation in the proximal small intestine. *J. Biol. Chem.* **282**: 1518–1528.
49. Brites, P., H. R. Waterham, and R. J. Wanders. 2004. Functions and biosynthesis of plasmalogens in health and disease. *Biochim. Biophys. Acta.* **1636**: 219–231.
50. Terova, B., G. Petersen, H. S. Hansen, and J. P. Slotte. 2005. *N*-Acyl phosphatidylethanolamines affect the lateral distribution of cholesterol in membranes. *Biochim. Biophys. Acta.* **1715**: 49–56.
51. McFarland, M. J., E. A. Terebova, and E. L. Barker. 2006. Detergent-resistant membrane microdomains in the disposition of the lipid signaling molecule anandamide. *AAPS J.* **8**: E95–E100.
52. Moesgaard, B., J. W. Jaroszewski, and H. S. Hansen. 1999. Accumulation of *N*-acyl-ethanolamine phospholipids in rat brains during post-decapitative ischemia: a ³¹P NMR study. *J. Lipid Res.* **40**: 515–521.
53. Hansen, H. S., B. Moesgaard, H. H. Hansen, and G. Petersen. 2000. *N*-Acylethanolamines and precursor phospholipids—relation to cell injury. *Chem. Phys. Lipids.* **108**: 135–150.
54. Guan, X. L., X. He, W. Y. Ong, W. K. Yeo, G. Shui, and M. R. Wenk. 2006. Non-targeted profiling of lipids during kainate-induced neuronal injury. *FASEB J.* **20**: 1152–1161.
55. Hansen, H. H., C. Ikonomidou, P. Bittigau, S. H. Hansen, and H. S. Hansen. 2001. Accumulation of the anandamide precursor and other *N*-acylethanolamine phospholipids in infant rat models of *in vivo* necrotic and apoptotic neuronal death. *J. Neurochem.* **76**: 39–46.
56. Pike, L. J., X. Han, K. N. Chung, and R. W. Gross. 2002. Lipid rafts are enriched in arachidonic acid and plasmeneylethanolamine and their composition is independent of caveolin-1 expression: a quantitative electrospray ionization/mass spectrometric analysis. *Biochemistry.* **41**: 2075–2088.

ERRATA

An affiliation for Dr. Daniele Piomelli, Italian Institute of Technology, was inadvertently omitted on the following papers Dr. Piomelli co-authored:

Identification of biosynthetic precursors for the endocannabinoid anandamide in the rat brain. *J. Lipid Res.* 2008. 49: 48–57.

Pitfalls and solutions in assaying anandamide transport in cells. *J. Lipid Res.* 2010. 51: 2435–2444.

Plasma lipidomics reveals potential prognostic signatures within a cohort of cystic fibrosis patients. *J. Lipid Res.* 2011. 52: 1011–1022.

The omitted affiliation has now been added to the online versions of these papers.